A study of the symmetry properties and multi-state nature of perovskite oxide-based electrical pulse induced resistance-change devices

2006 New J. Phys. 8 229

(http://iopscience.iop.org/1367-2630/8/10/229)

New Journal of Physics
The open–access journal for physics

A study of the symmetry properties and multi-state nature of perovskite oxide-based electrical pulse induced resistance-change devices

X Chen[1], J Strozier, N J Wu, A Ignatiev and Y B Nian
Center for Advanced Materials, University of Houston,
Houston, TX 77204, USA
E-mail: xchen7@uh.edu

New Journal of Physics **8** (2006) 229
Received 16 May 2006
Published 9 October 2006
Online at http://www.njp.org/
doi:10.1088/1367-2630/8/10/229

Abstract. A new symmetric two-terminal non-volatile electrical pulse induced resistance-change (EPIR) device is fabricated in the $Pr_{0.7}Ca_{0.3}MnO_3$ (PCMO) materials system and analysed. Two actual devices of somewhat different construction are tested. Both consist of two similar half-parts, characterized by similar resistance versus pulse voltage hysteresis loops, which are reversely connected together in series forming a reflection symmetric device. Even though the devices are as physically symmetric as possible, they are found to exhibit resistance-switching under the application of voltage pulses of different amplitude and of different polarities. A symmetric model of the above device is proposed, and its analysis confirms the features noted above. The switching is history dependent and shows multi-intrinsic state resistance switching, which is very useful for developing future multi-bit EPIR devices.

[1] Author to whom any correspondence should be addressed.

PII: S1367-2630(06)24546-4

Contents

1. Introduction

The observation of the electrical pulse induced resistance-change (EPIR) effect [1] in perovskite oxide thin films such as $Pr_{0.7}Ca_{0.3}MnO_3$ (PCMO) at room temperature has drawn much attention [2]–[4]. Usually the device is constructed as a thin PCMO film (of around 500 nm thickness) sandwiched between two electrodes. The resistance of the device can be switched down by a short electric pulse of one polarity and switched up by a short pulse of the opposite polarity. Such simple structured resistive switching devices have important application in novel non-volatile high-density memories [2, 5, 6].

However, the basic mechanism responsible for the EPIR effect is still under investigation. Switching of the resistance of such an electric device by reversing the polarity of the switching pulse has brought into question the conservation of parity [7]. This question has resulted in much discussion [8, 9] with suggestions that a necessary requirement for EPIR switching is an asymmetry resulting from device fabrication, and that the EPIR effect cannot be an intrinsic property of the PCMO that constitutes the bulk material of the device [7]. It should be noted that the EPIR switching effect appears not only in asymmetric devices with two different electrodes, but also in symmetrically looking devices such as a PCMO thin film sandwiched between two similar electrodes. It has been further suggested, based on dielectric constants arguments, that the effect is limited to an interfacial layer not thicker than 10 nm, and the two interfaces of the device are quite different from fabrication even before any pulsing [7, 10].

Recent study, however, has shown that not only is the dielectric constant in PCMO at room temperature much larger [11] than the earlier estimation, calling into question the projected interface layer thickness [7], but the active region is also much larger—100 nm or more extended into the bulk from the electrode/perovskite oxide interface [12]. In addition, there is also recent evidence of possible switching in the bulk material itself [9, 13].

It now remains to be seen if an asymmetry in the construction of an EPIR device is required for resistance switching. To investigate the role of symmetry, or lack of it, in the EPIR effect, we have carefully constructed a resistance-switching device to be as physically symmetric as possible within the constraints of sample preparation. The device consists of two more-or-less identical half-parts connected together in mirror image series. The two parts not only are structurally similar, but also have very similar resistance switching characteristics as given by their resistance versus voltage hysteresis curves.

Fabricated symmetric devices were subjected to electrical pulses of different voltage amplitudes and polarity, and the resulting hysteresis curves of the devices indeed showed resistance switching.

These results were analysed in terms of a theoretical idealized resistance model that was designed to be completely symmetric. The good agreement between experimental results of the real device, and the calculations using the idealized model, indicates that a symmetric device (one having mirror image symmetry) can indeed switch if there are certain constraints on the voltage amplitude of the applied switching pulses. This result is important for future memory device development.

2. Fabrication of two symmetric switching device and experimental results

Two actual symmetrically structured EPIR devices were constructed, and each was characterized by measuring its total resistance as a function of switching pulse amplitude (both positive and negative), with the result plotted as a device hysteresis loop.

The first device (figure 1(a)) consists of two half-parts, each half-part consisting of a vertical layered structure of a silver (Ag) top electrode, a PCMO layer and a $YBa_2Cu_3O_{7-x}$ (YBCO) bottom electrode. The device is fabricated by pulsed laser deposition (PLD) on a $LaAlO_3$ (LAO) substrate as initially described by Liu *et al* [1]. The PCMO films are approximately 3 mm $\times$ 4 mm, and the two haft-parts are connected together through the common YBCO bottom electrode. In addition to the top Ag electrodes, an Ag contact is also made to the exposed area of the YBCO bottom electrode surface. The Ag electrode pads, which are approximately 0.4 mm in diameter, are sputtered on top of the PCMO and YBCO films, and are later connected to Ag wires with silver paste for connection to the testing circuit.

An Agilent 8114A Pulse Generator was used to send electrical pulses to the sample. Square pulses of 200 ns duration with varying amplitude and polarity were used to switch the sample resistance. The pulse shape was monitored with a Tektronic TDS 520 Digitizing Oscilloscope. After each pulse, the sample was connected to a resistance measurement circuit, which applied a 1 μA current to the sample by a Keithley 200 Programmable Current Source, and measured the voltage drop across the sample with a Keithley 617 Programmable Electrometer. The two half-parts were first tested to confirm that they are very close in switching behaviour to one another, and then the whole device was put under test and the switching hysteresis loop of the complete device was experimentally determined. The experiment was performed in air at room temperature. The resistance of the device was observed to be switched after the electric pulses were applied, and the resistance was stable after switching. The results are shown in figure 1(b).

Contrary to the earlier suggestions, this symmetric device does show resistance switching. The hysteresis loop in figure 1(b) has a characteristic two-lobe structure and will be compared later to a model simulation for a symmetric device. The observed switching is related to the symmetric structure of the device, negating the suggestion that a built in asymmetry in the device, even before any pulsing, is a critical requirement for switching in the EPIR device. The resistance of the half devices during the testing of figure 1(b) is measured and plotted in figure 1(c), where the square symbols and the —— indicate the resistance of the left half, and the circle symbols and the - - - - indicate the right half. The □ and ○ are the data for the voltage

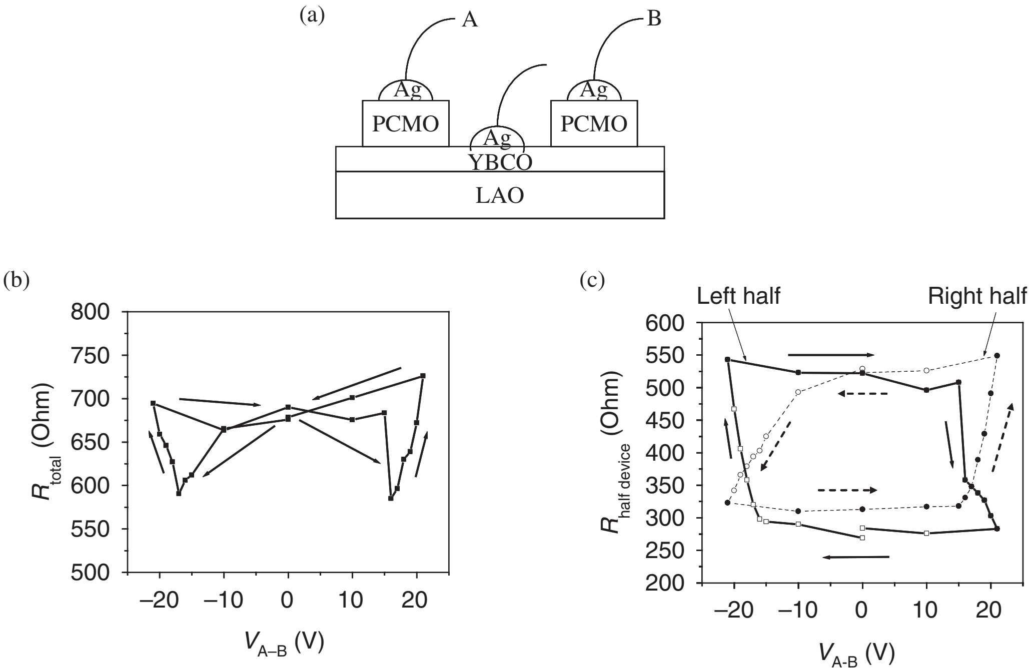

Figure 1. The experimental hysteresis loop of an actual EPIR device with a symmetric structure: (a) a schematic of the symmetric device; (b) the resistance versus pulse voltage loop for the total device; (c) the resistance versus pulse voltage of each of the two half devices during the test. (Each resistance was measured after the pulses voltage was applied.)

scan from positive to negative, where with −15 to −22 V pulses applied to the device A–B, the right half resistance gradually switched down from the high state of ∼500 Ω to the low state of ∼300 Ω, and with voltage pulse larger than −15 V the left half resistance gradually switched up from the low state of ~ 300Ω to the high state of ∼500Ω, with the switching down happening a little earlier, so that the total device resistance switched down first and then switched back to the high value of R_{total}. This agrees with the data shown in figure 1(b). Note when a half device resistance is being switched, it does not jump directly from low state to high state or jump from high state to low state, but shows intermediate resistance levels under pulses with increasing amplitudes. As seen in the figure, the half device resistance changes gradually with increasing pulse amplitude (greater change with higher pulse amplitude), indicating that any resistance value between the high and low states can be obtained for the half device by choosing a proper switching voltage. The ■ and • in figure 1(c) are the data for the voltage scan from negative to positive, where with +15 to +22 V pulses applied to the device, the left half switched down and the right half switched up, with the switching down happening earlier, so that R_{total} switched down first and then switched back to the high value as seen in figure 1(b). In figure 1(c) it is seen that the switching behaviours of the two halves are nearly mirror images of each other, supporting the symmetric nature of the fabricated device and confirming that symmetry is involved in the full device switching behaviour. The sum of the half device resistances in figure 1(c) is slightly larger than the R_{total} value in figure 1(b) due to the nonzero contact resistance between Ag and YBCO.

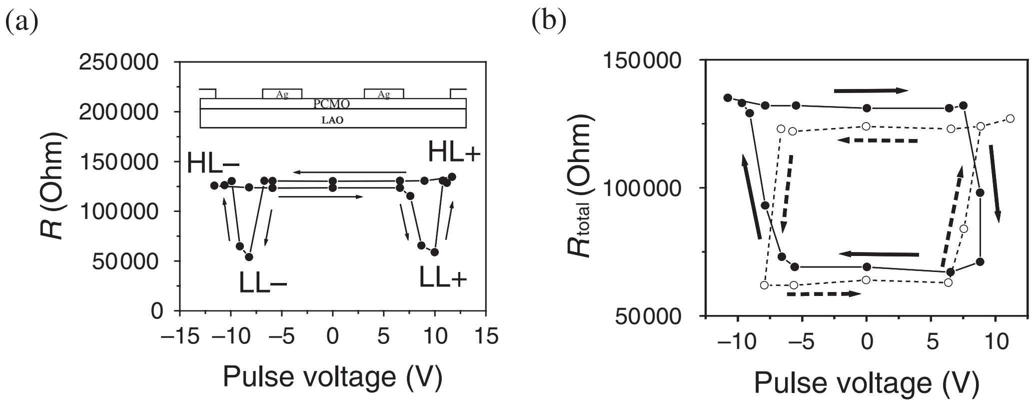

Figure 2. (a) The 'table with legs' symmetric switching loop obtained on a microfabricated EPIR device (insert is the device structure); (b) The asymmetric hysteresis curve of the micro-fabricated device obtained at the voltage range of −9 to +12 V and the voltage range of −12 to +9 V.

The second symmetric device was fabricated from a approx. 200 nm thick PCMO thin film, which was grown on an 5 mm × 10 mm sized insulating LAO substrate by PLD and lithographically patterned into a 40 μm wide stripe. Ag electrodes of 100 μm width and approx. 20 μm separation were deposited on top of the PCMO stripe by DC-sputtering and lithographic processing (schematically shown in the insert of figure 2(a)). Figure 2(a) gives the pulse switching hysteresis loop of the micro-fabricated device indicating that this symmetric device also shows resistance switching. The hysteresis loop of figure 2(a) is similar in shape to that of figure 1(b), and exhibits the two-lobed 'table with legs' type diagram, which is characteristic of such a symmetric device and is distinguished from the hysteresis loops of asymmetric EPIR devices. Certain regions on the R versus pulse voltage curve in figure 2(a) are more-or-less horizontal, indicating that little or no resistance switching is taking place. Other regions have a steep R versus pulse voltage slope with respect to the horizontal axis and indicate a 'transition region' in which the resistance is switched by the applied pulses. For convenience, we have labelled the characteristic resistance states in the figure 2(a) as HL+, HL−, LL+ and LL− states, which will be further addressed later.

The hysteresis data from these two actual devices demonstrates that mirror symmetrical devices can exhibit resistance switching within certain pulse amplitude conditions. Although as can be seen from figure 2(a), there is no difference in the total resistance and hence no net resistance switching of a perfectly symmetric resistive device when pulsed with saturating pulses of opposite polarities, this does not preclude switching when pulses of different amplitudes are applied. To demonstrate this, we undertook resistance switching under restricted pulse voltage ranges. In particular for the second device, the ○ and - - - - of figure 2(b) show the device hysteresis loop obtained using a pulse voltage range of from about −9 to +12 V, in which the device showed resistance switching up to larger values under positive pulsing and switching down under negative pulsing, while as shown in figure 2(b) by the • and ——, using a pulse voltage range of from about −12 to +9 V, the device showed reversed switching polarity: switching up under negative voltage pulsing and switching down under positive voltage pulsing. In figure 2, it is observed that reducing the voltage at the bottom of the 'transition region' results in a horizontal line

Table 1. The switching of resistance elements at different states of the planar device.

Pulse Voltage (V)	State	R_R (kΩ)	R_F (kΩ)	R_L (kΩ)	R (kΩ)
8.7	LL+	19.8	0.8	46.7	65.5
11.7	HL+	105.5	0.8	27.4	134.4
−8.2	LL−	25.6	0.6	28.4	53.9
−10.6	HL−	24.5	1.7	104	126.2

(no switching) that continues across to the bottom of the transition region of the opposite polarity, instead of going back in the transition region where the resistance has been switched down. This suggests that resistance switching by the short switching pulses is thermodynamically irreversible and might be of first order.

The resistance elements in the planar device of figure 2 with the device in the HL+, HL−, LL+ and LL− states were also measured by the four-point resistance method and listed in table 1, which shows the variation of the resistance of the device R, and the three individual resistance regions: R_L the resistance of left interface region near the electrode, R_R the resistance of right interface region near the electrode, and R_F the resistance of the PCMO film between the electrode regions. The four-point resistance results in table 1 show that roughly 98% of the switching occurs in the interface region while, 2% is a bulk phenomena. These results have been further confirmed by direct scanning Kelvin probe microscopy resistance profile analysis [13].

3. Symmetric device modelling

3.1. Symmetric device model

For analysis, we chose as a theoretical model an idealized device that has reflection (mirror image) symmetry. Figure 3(a) showed the schematic of a model symmetric device consisting of two identical half-parts, which was used for the numerical simulation of the device. The left half of the device, A–O, consists a top terminal electrode A in contact with a functional oxide switching layer, which is made on a bottom electrode. A reference electrode O is connected to the bottom electrode. The right half-part of the device B–O is structurally identical to the left half, A–O.

Either of the two half-devices can be viewed as a two-electrode device, which is not symmetric. We propose a resistance switching hysteresis behaviour of the left half-device as shown in figure 3(b). For simplicity, we have assumed that in the transition region, the half-device resistance varies linearly with the pulse voltage drop across it, and that switching does not take place for decreasing pulse amplitude. For the resistance switch hysteresis loop of R_{A-O}, the resistance across A–O is affected by the applied pulse from A to O (V_{A-O}). An increasing positive pulse voltage V_{A-O} of 5–6 V is assumed to gradually switch R_{A-O} from 10 Ω down to 5 Ω, and a negative voltage of −5 to −6 V gradually switch R_{A-O} up from 5 to 10 Ω. For voltage between 5 and 6 V, and between −5 and −6 V, the half device resistance has resistance values between 5 and 10 Ω following the resistance versus pulse voltage curve in the figure. The right half-device, B–O, is identical to the left half-device, however, by setting the positive direction in the O–B direction, the right half-device B–O shows a similarly shaped,

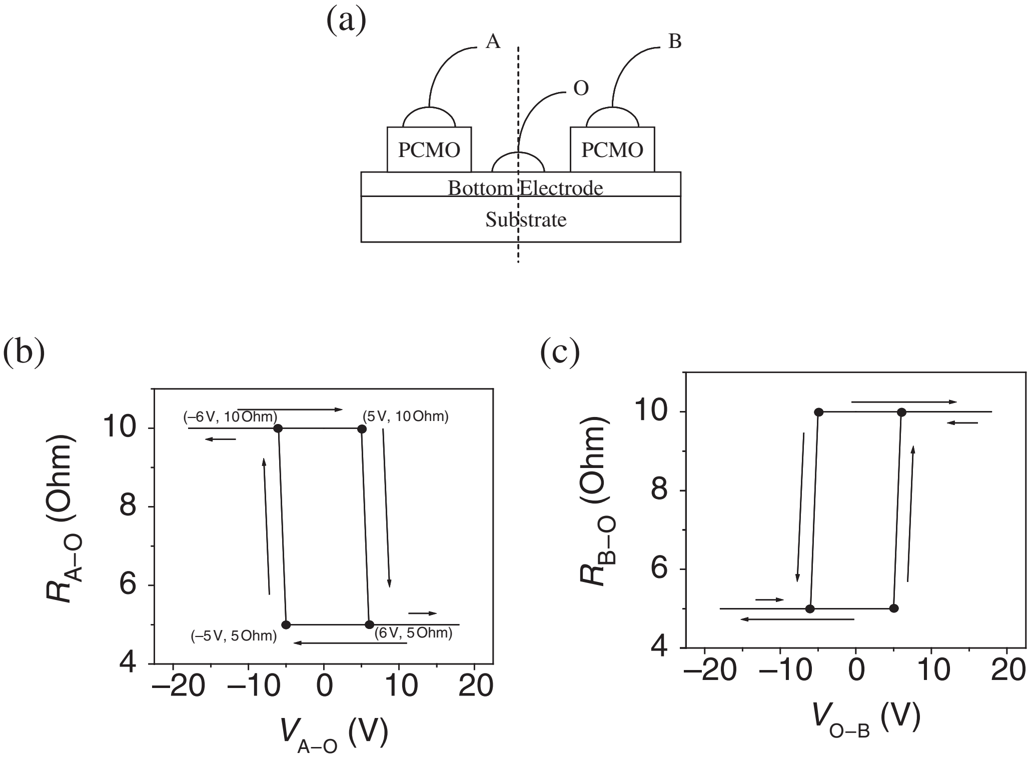

Figure 3. (a) a schematic of the modelled symmetric device; (b) the switching hysteresis loop of the half device A–O ($V = V_{A-O}$, $R = R_{A-O}$), which is mirror image of (c) the loop of half device O–B ($V = V_{O-B}$, $R = R_{B-O}$).

but mirror image hysteresis loop R_{B-O} versus V_{O-B} to that of the left half A–O as shown in figure 3(c).

Figure 4 shows a computer simulation of the hysteresis curve of resistance versus pulse voltage for the whole two terminal A–B device. Note that to obtain the whole device the two MIRROR halves are connected in series, i.e. A–O is connected to O–B. In calculating the applied pulse voltage that causes the switching, we calculate the voltage across each of the half-devices taking into account the resistance of each of the two parts. Obviously switching history is important in determining the voltage across each half at each point in the hysteresis curve, and this fact is built into the computer simulation.

We begin the computer simulation with both half-devices in the high resistance state. For the full device, the pulse voltage ranges between ±18 V and is increased (or decreased) by 0.5 V for each point on the curve, producing the hysteresis curve of figure 4. The points numbered 1 through 11 and the arrowheads indicate the resistance states and the switching sequence in the hysteresis loop. The starting point is labelled as the HH state, indicating both halves are in high resistance state. When the switching is stabilized, the characteristic HL+, HL−, LL+ and LL− resistances states of figure 2(a) are reproduced in the modelling and are labelled in figure 4. The model results show that the HL± states are with one half high and the other half low in resistance, and the LL+ and LL− states are identical with both halves low in resistance. In the cycle, points 3 through 11 reproduce the unique 'table with legs' shaped hysteresis loop of figure 2(a). Note that in this cycle there are more than just two high and low ('on' and 'off') resistance states.

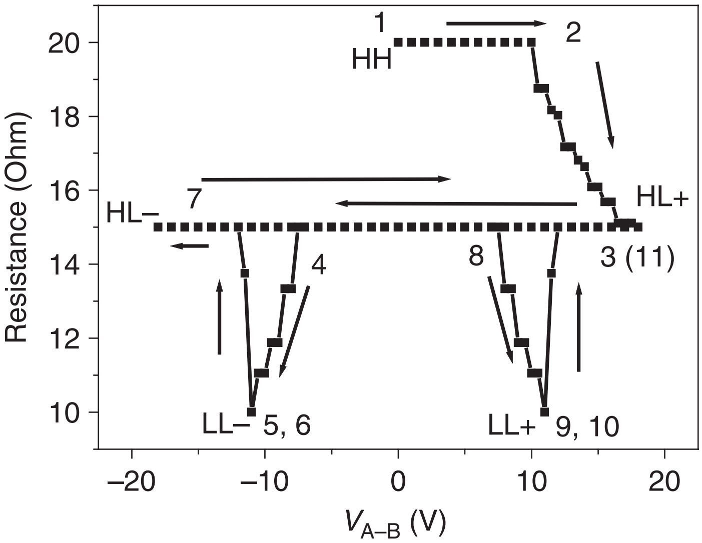

Figure 4. The switching of the symmetric device, which has 'symmetrical' half device hysteresis loops.

Although both HL+ and HL− are at 15 Ω, they are different states of the device that are mirror to each other and respond differently to external pulses. This simulation clearly confirms that a symmetrically constructed EPIR device can indeed switch resistance if the switching pulses are within certain limits.

As we have experimentally observed, a half-device is asymmetrical, and generally the switching up voltage for R_{A-O} begins at a different amplitude from the switching down voltage. To examine this general result, the model was changed such that the starting negative switch voltage was −7 V and the saturating negative switching voltage was −8 V. Thus the starting and saturating negative switch voltages have different absolute values from the corresponding positive switch voltages. The hysteresis loop of this device in the full voltage range is shown in figure 5(a) and is very similar to that of figure 4. In these 'table with legs' hysteresis loops, the switching voltages are well defined, similar to that of the half devices, so that the symmetric device can be easily used in actual applications.

The resistance change of each of the two-half devices of figure 5(a) as a function of pulse voltage V_{A-B} is shown in figure 5(b), and it is seen that their switching behaviours are mirror images of each other, similar to the experimental observation in figure 1(c).

We also calculated the bi-polar switching characteristics of the modelled device under selected pulse voltages, which are shown in figure 5(c). We first use a large positive voltage pulse across A–B (first training) to set the device to the HL+ state, and then we subject the device to alternate positive and negative pulses. As shown in the figure, we can switch the device resistance R_{A-B} back and forth between 15 and 10 Ω with alternate +16 and −13 V pulses. We can then apply a large negative V_{A-B} (second training) and then again apply alternate +13 and −16 V pulses to the device with R_{A-B} switching back and forth between 10 and 15 Ω. Note the device now switches to the low resistance state with positive pulses and to the high resistance state with negative pulses, which is opposite switching polarity to that seen after the first training. This result indicates the direction of resistance change under switching polarity can be controlled in an EPIR device.

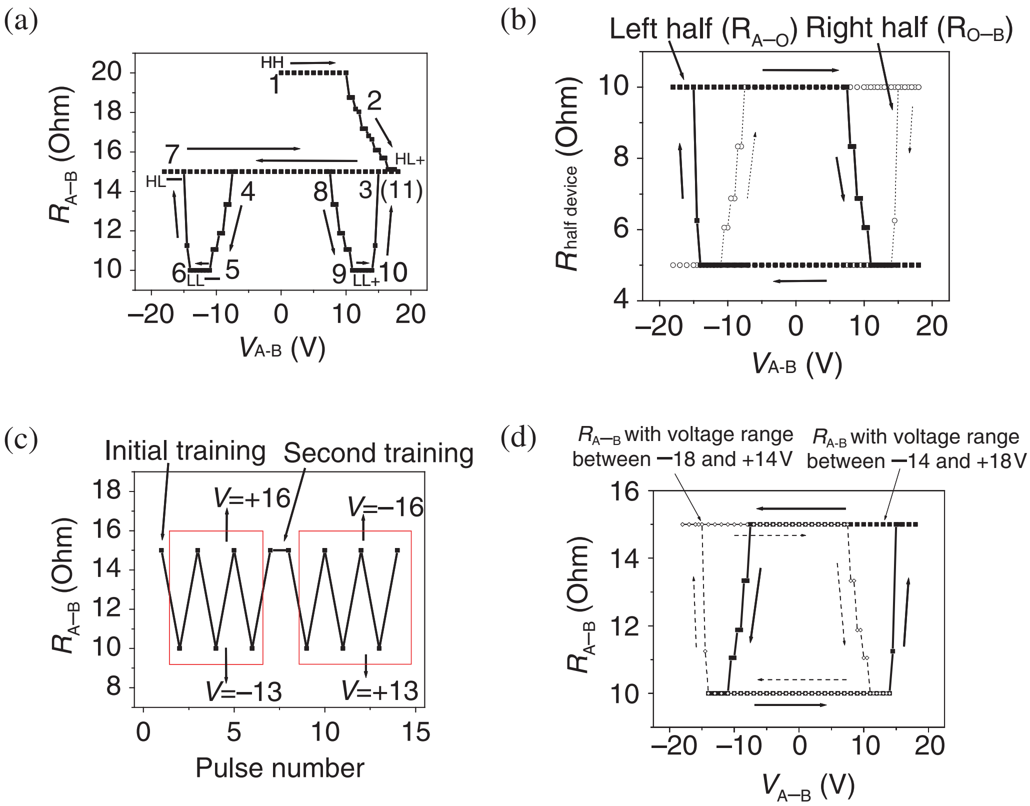

Figure 5. Computer calculations on the structurally symmetric device A–B: (a) the symmetric 'table with legs' switching hysteresis loop (point 3–11) is reproduced from the simulation; (b) the hysteresis curves of the half devices during the test of (a); (c) bi-polar like switching behaviour of A–B after training with a single voltage pulse: initial training +20 V, second training −20 V; (d) the asymmetric hysteresis curve of A–B obtained from a restricted voltage range (the apparent asymmetry can be reversed by using a different voltage range).

The polarity dependant switching behaviour seen in figure 5(c) can also be demonstrated in the switching hysteresis loop test. As shown in figure 5(d), scanning pulse voltages between −14 and +18 V will result in a resistance switching loop in which a positive pulse switches R_{A-B} up, and a negative pulse switches R_{A-B} down. Scanning pulse voltages between −18 and +14 V will result in a hysteresis loop of the opposite polarity.

3.2. Symmetric device model fitting experimental results

Figure 6 shows the result of a simulation where we used a small fixed resistance to represent the bulk of the PCMO film, and two switchable interface resistances to represent the two Ag/PCMO interface region resistances. The two interfaces are mirror to each other in the device. By adjusting the switching element parameters, we obtained the result shown in figure 6(a) (the small switching contribution from the bulk is neglected here, but will be addressed elsewhere). The solid curve in the figure is the R versus pulse voltage loop obtained under full pulse voltage ranges, which is quantitatively in good agreement with the experimental results of figure 2(a). We further

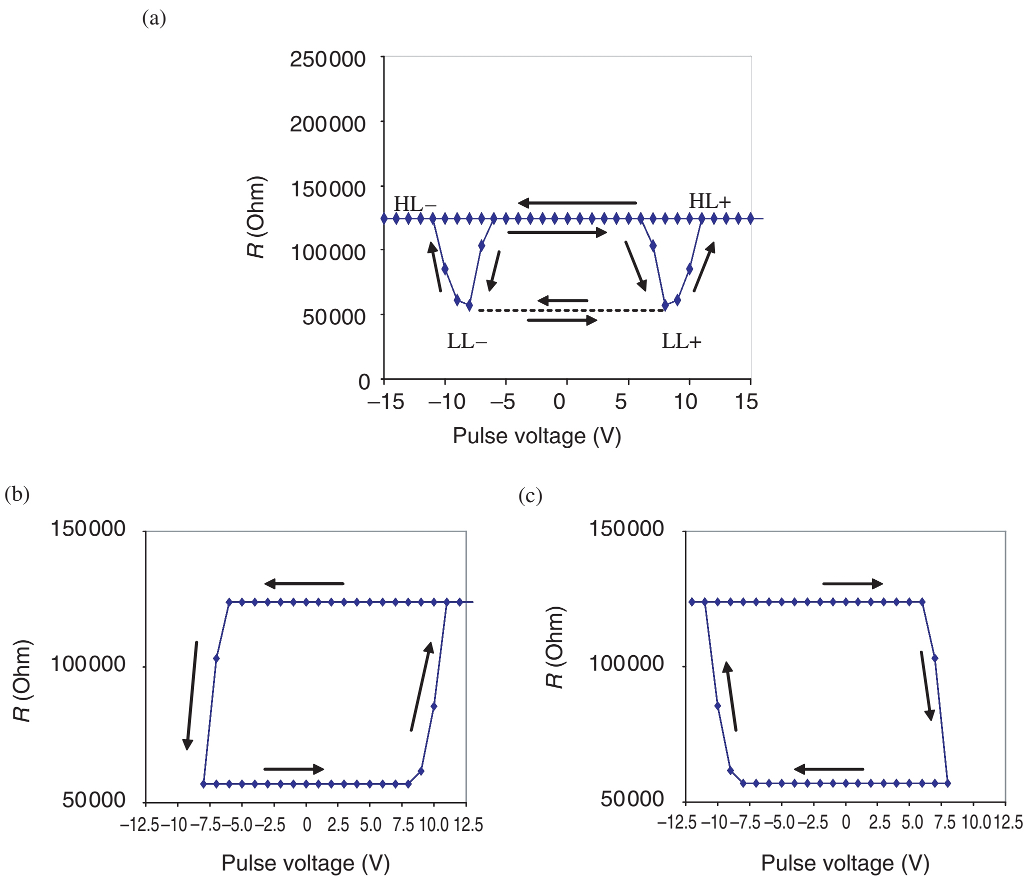

Figure 6. A simulation result that is quantitatively agree with the experimental results in figure 2; (a) a theoretical simulation of the symmetric device switching hysteresis in the full voltage range; panels (b) and (c) in different restricted voltage ranges.

simulated the switching under the partial voltage ranges, with the results shown by the - - - - in the R versus pulse voltage curve of figure 6(a). A clearer representation is shown in figure 6(b) and (c), where applied pulses with small negative amplitude and large positive amplitude will result in a polar-like switching where positive pulses switch the device resistance up and negative pulses switch the device resistance down as seen in figure 6(b). Applied pulses with large negative amplitude and small positive amplitude will result in a different polar-like switching where positive pulses switch the device resistance down and negative pulses switch the device resistance up as seen in figure 6(c). These results are also quantitatively in good agreement with the experimental results in figure 2(b).

3.3. A summary of the symmetrical model

The model discussed in the above sections has confirmed the symmetric EPIR device properties. This new model is started with two completely identical half parts, which are reversely connected together. It is found that the physically symmetric M–PCMO–M device can exhibit resistance switching under the application of voltage pulses of different amplitude and of

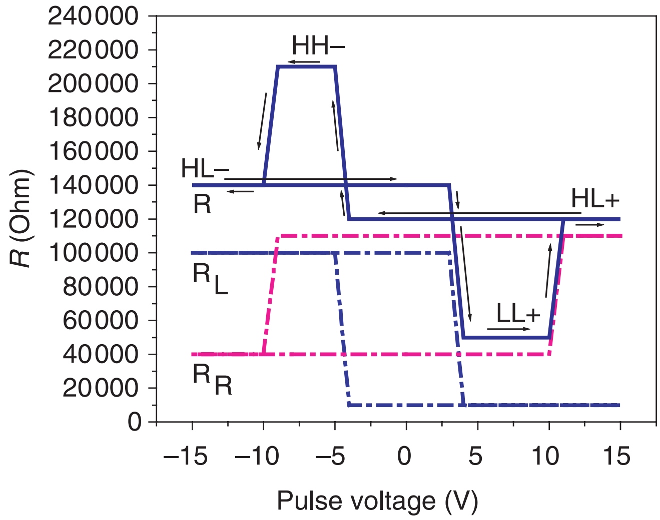

Figure 7. A schematic modelled hysteresis loop test demonstrating multi resistance level switching in a multi element EPIR device.

varying polarities and show a symmetric switching hysteresis loop. Two restricted voltage range resistance hysteresis loops of the device that are polar-like by themselves, but are mirror image of each other, can be obtained by selecting different voltage ranges as seen in figure 5(d), figure 6(b) and (c).

4. Multi-switching element property applications

Finally, there is another important prospective from the multi switching element nature of the EPIR device: it can be used to develop future multi state memory devices. The symmetric device as in figure 6(a) can be switched to three different intrinsic memory states based on the high and low states of its two interfaces: HL−, HL+ and LL± states. More states can be demonstrated in an EPIR device if we include the bulk resistance switching. For practical device application, it is not limited to be a symmetric device. Understanding the multi-element and multi-state nature, and knowing that the resistance switching of the different elements does not need to happen at the same time, we can design and fabricate an EPIR device in which all the states are different in resistance as shown in figure 7. Here we model R_L with a smaller switching voltage than R_R. Both interface regions having different high and low resistance values. Under a small negative voltage, R_L is switched up and the device goes to HH− state (with both interface high in resistance); under a high negative voltage, R_R is switched down and the device goes to HL− state; under a small positive voltage, R_L is switched down and the device goes to LL+ state; and under a high positive voltage, R_R is switched up and the device goes to HL+ state. The switching of the two interface resistances can result in a two-bit device with four distinct memory states: HH−, HL−, HL+, and LL+ state. We have recently observed similar behaviour by changing the oxygen concentration in a PCMO thin film grown on Pt/TiN/SiO_2/Si substrates [14]. Furthermore, engineering different resistance switching parameters and values of the two interfaces and the bulk resistance may generate more states for the EPIR device. The modelling presented in this paper, although very simple, is demonstrated to be a very powerful tool for studying the EPIR effect.

5. Discussion of the symmetry issue

The symmetry question for an EPIR device has been addressed here and clarifies a controversy in EPIR research that alleges a violation of a fundamental law of physics: the conservation of parity [7].

As an EPIR device is an electrical device, we expect that parity conservation should hold for such a device. It is intuitive to think that if a device is originally constructed to be symmetrical, there should be no resistance switching; conversely, if resistance switching is observed, the device must be constructed to be asymmetrical. However, this study demonstrates that asymmetry in the construction of the device is not necessary for resistance switching, as long as the switching voltages are within certain limits (e.g., one at saturation, and the other in some narrow range less than saturation). The study presented in this paper clearly shows that an EPIR device that is constructed symmetrically can still exhibit resistance switching.

Some of the important results are:

1. The EPIR effect is not limited to resistance switching at only one of the two interfaces between the metal electrodes and PCMO. Our results clearly show resistance switching at both of the interfaces of the device under certain values of the switching voltage, can result in overall resistance switching of the device. There is also an addition of resistance switching in the bulk [9, 13] of the PCMO thin film.
2. The resistance switching in an EPIR device does not necessarily have to be polar. This is shown for the experimental results in figure 2(a) and the simulation in figure 6(a).
3. A symmetrically constructed device can show a polar-like switching behaviour under certain conditions such as shown in figure 6(b) depending on switching voltage history.

6. Conclusions

We have demonstrated, both by experiment on fabricated structurally symmetric EPIR devices, and by simulation using an ideal symmetric model, that multi-state resistive switching in a structurally symmetric EPIR device is possible under certain well-defined pulsing conditions. We have also found an important feature of a symmetric EPIR device: its switching polarity can be selected and engineered simply by controlling pulsing conditions. These properties indicate the EPIR devices presented here have application as multi-state resistive memory devices.

After demonstrating a symmetric device can switch, it is still to be resolved as to exactly how the resistance of an oxide material sandwiched between two metal electrodes is hysteretically switched under the application of short electric pulses. We have recently performed some research on this topic, which will be published elsewhere [14].

Acknowledgments

Assistance from A Zomorrodian, C Papagianni, L Smith, Y Song, and Z W Xing is greatly acknowledged. This study was partially supported by NASA, the State of Texas through the Center for Advanced Materials, Sharp Laboratories of America, and the R A Welch Foundation.

References

[1] Liu S Q, Wu N J and Ignatiev A 2000 *Appl. Phys. Lett.* **76** 2749
[2] Zhuang W W *et al* 2002 *Tech. Dig.—Int. Electron Devices Meet. 2002* 193–196
[3] Dagotto E 2005 *Science* **309** 257
[4] Dagatto E 2005 *New J. Phys.* **7** 67
[5] Tokura Y 2003 *Phys. Today* **56** 50
[6] Pinnow C U and Mikolajick T 2004 *J. Electrochem. Soc.* **151** K13
[7] Baikalov A, Wang Y Q, Shen B, Lorenz B, Tsui S, Sun Y Y, Xue Y Y and Chu C W 2003 *Appl. Phys. Lett.* **83** 957
[8] Rozenberg M J, Inoue I and Sanchez M J 2004 *Phys. Rev. Lett.* **92** 178302
[9] Aoyama K, Waku K, Asanuma A, Uesu Y and Katsufuji T 2004 *Appl. Phys. Lett.* **85** 1208
[10] Tsui S, Baikalov A, Cmaidalka J, Sun Y Y, Wang Y Q, Xue Y Y, Chu C W, Chen L and Jacobson A J 2004 *Appl. Phys. Lett.* **85** 317
[11] Mercone S, Wahl A, Pautrat A, Pollet M and Simon C 2004 *Phys. Rev.* B **69** 174433
[12] Chen X, Wu N J, Strozier J and Ignatiev A 2006 *Appl. Phys. Lett.* **89** 63507
[13] Chen X, Strozier J, Wu N J and Ignatiev A 2005 *Appl. Phys. Lett.* **87** 233506
[14] Nian Y B, Strozier J, Wu N J, Chen X and Ignatiev A 2006 *Preprint* cond-mat/0602507